JOURNAL OF SOLID STATE CHEMISTRY 97, 74–81 (1992)

The Aragonite-Type Neodymium Borate $NdBO_3$: Energy Levels, Crystal Field, and Paramagnetic Susceptibility Calculations

ELIZABETH ANTIC-FIDANCEV,* JILALI ARIDE,†,‡
JEAN-PIERRE CHAMINADE,† MICHÈLE LEMAITRE-BLAISE,*
AND PIERRE PORCHER*

Laboratoire des Eléments de Transition dans les Solides, UPR 210 du CNRS 1, Place A. Briand, 92195 Meudon Cédex, France; †Laboratoire de Chimie du Solide du CNRS, 351 Cours de la libération, 33405 Talence Cédex, France; and ‡Ecole Nationale Supérieure, Avenue Oued Akreuch, BP 5118 Rabat, Morocco

Received May 22, 1991; in revised form September 6, 1991

Optical absorption spectra of $NdBO_3$ single crystals were measured between 3900 and 31,700 cm^{-1} at liquid helium to room temperature. The derived energy level scheme with 119 levels was simulated according to the crystal field theory including free ion effects yielding a rms deviation of 15 cm^{-1}. The 14 free ion and 14 crystal field parameters allowed by the C_s symmetry of the neodymium site were calculated. The derived wavefunctions were used in calculating the paramagnetic susceptibility and its variation with the temperature between 4.2 and 500 K by the van Vleck formula. Experimental and calculated values are in good agreement. © 1992 Academic Press, Inc.

The rare earth orthoborates $REBO_3$ constitute a family of compounds isostructural with the calcium carbonate mineral $CaCO_3$. The low temperature forms of these compounds are not, however, isomorphous along the whole *RE* series. From lanthanum to neodymium, the borates have the orthorhombic aragonite type of structure, but from samarium to lutecium, the rhombohedral vaterite type prevails. The lutetium borate has also the trigonal calcite type. The three varieties of the mineral $CaCO_3$ are thus found for the borate family.

The optical properties of $ScBO_3$, $PrBO_3$, $REBO_3$ (Sm–Yb, Y) have been studied by IR and Raman spectroscopy (*1*, *2*) and by emission spectroscopy of Eu^{3+} embedded in both calcite- and vaterite-type $LuBO_3$ (*3*). The luminescence properties of Bi^{3+} in the three structural types of $REBO_3$ have also been reported (*4*).

The purpose of this paper is to present the absorption spectra of the orthorhombic $NdBO_3$ and to simulate the energy level scheme according to the crystal field theory. The derived wavefunctions are employed to calculate the paramagnetic susceptibility and its variation as a function of temperature.

I. Crystallographic Background

The structure of neodymium borate belongs to the orthorhombic space group *Pnam* (No. 62) isomorphic with the aragonite mineral $CaCO_3$. The unit cell dimen-

0022-4596/92 $3.00

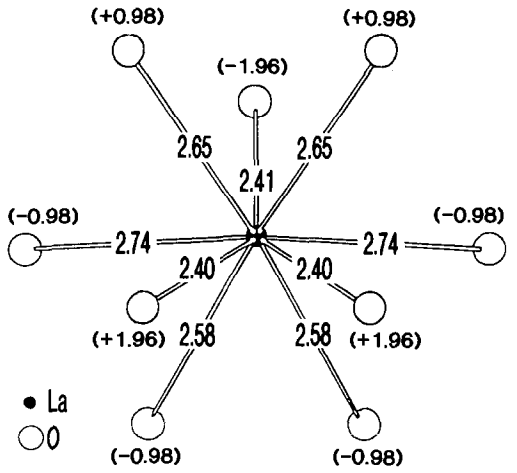

FIG. 1. Lanthanum environment in $LaBO_3$ (*6*). Distances in Å units.

sions obtained for our sample (a = 5.725, b = 5.031, and c = 8.074 Å) are close to the values given by Levin *et al.* (*5*). The neodymium occupies a single site with C_s point symmetry with coordination number nine. Figure 1 shows the environment of the lanthanum in $LaBO_3$ (*6, 7*). The La–O distances vary between 2.40 and 2.74 Å. The bond length of 2.40 Å is close to the distance found in the $(LnO)_n^{n+}$ complex cation found in a number of rare earth compounds (e.g., in oxyhalides, tungstates, molybdates, sulfates, etc.). This complex cation is known for its very covalent character (*8, 9*). Though there is no clear correlation between the rare earth borates and the oxyhalides, this feature can explain why electrostatic point charge calculations of the crystal field parameters were not successful.

II. Experimental

The absorption measurements were performed at liquid helium, 10 K, liquid nitrogen, and room temperature. The spectra were recorded on both a 3.4-m Jarrell–Ash grating spectrograph and on a 2400 Cary spectrophotometer in the UV, the visible, and the near-IR wavelength range from 3900 to 31,700 cm^{-1}. The upper wavenumber limit was restricted by the BO_3^{3-} absorption.

The paramagnetic susceptibility measurements and its variation with temperature were measured on a Faraday balance between 4.2 and 500 K on crushed $NdBO_3$ crystals.

III. Analysis of the Spectra

As expected from crystallographic results, the neodymium occupies a single site, with a low point symmetry, C_s. The absorption spectrum recorded at 4.2 K confirms this assumption with only one line for the well isolated $^4I_{9/2} \rightarrow {}^2P_{1/2}$ transition. The energy of the $^2P_{1/2}$ level in the nephelauxetic energy scale (*10*) situates in the ninefold coordination area of the neodymium salts, as is the case of $NdPO_4$ (*11*) with monazite structure. The 119 energy levels (from the 182 Kramers' doublets of the $4f^3$ configuration) are derived from absorption measurements essentially at low temperature. The room temperature absorption yields the $^4I_{9/2}$ ground level splitting: 0–99–145–288–588 cm^{-1}. Figure 2 represents the IR absorption spectrum from the ground level to $^4I_{15/2}$ at 10 K; all Stark levels could be attributed unambiguously, showing that very low temperature measurements are not absolutely necessary.

Several zero-phonon transitions have vibronic sidebands, especially those for which $\Delta J = 2$ as a consequence of their hypersentive character (*12*). For example, the $^4I_{9/2} \rightarrow {}^4G_{5/2}$, $(2G_{7/2})$ hypersensitive transitions (around 580 nm) show many vibronic lines corresponding to the B–O stretching frequencies at about 600, 940, and 1970 cm^{-1} (Fig. 3 and Table I). For transitions to the $^4F_{3/2}$, $^4G_{7/2}$, and $^2P_{1/2}$ levels other vibration frequencies are observed in the 100–200 cm^{-1} range, some of them not mentioned in Ref. (*1*). More precisely, around $^2P_{1/2}$, we found satellites at 107, 127, 144, 161, 201,

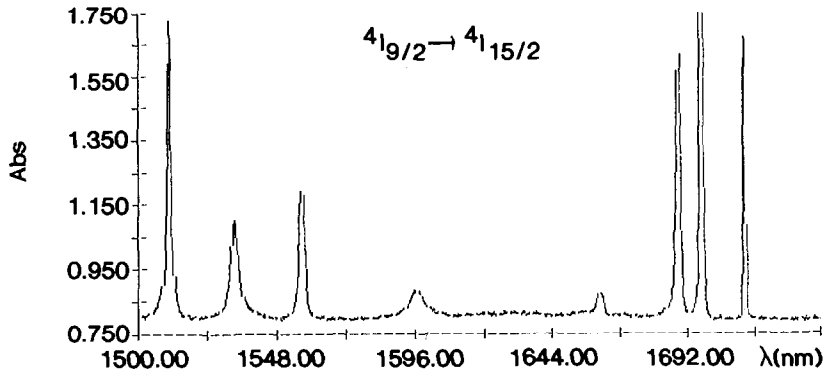

FIG. 2. Part of the absorption spectrum of $NdBO_3$ at 4.2 K.

and 221 cm^{-1}. The same series of vibronic transitions is recorded at 77 K. It is often difficult to recognize an electronic transition from a multitude of lines (*13, 14*) but all vibronic and electronic transitions could be attributed without any doubt.

IV. Energy Level Simulation

The simulation of an energy level scheme of considerable size can be carried out according to the crystal field theory, considering the central ion submitted to various interactions which are described by a sum of tensorial operator products.

(i) The free ion Hamiltonian includes various interactions whose magnitude is reproduced by 14 phenomenological parameters, among which the four Racah parameters, E^k, the spin-orbit coupling constant ζ, the three two-body (Trees') parameters (α, β,

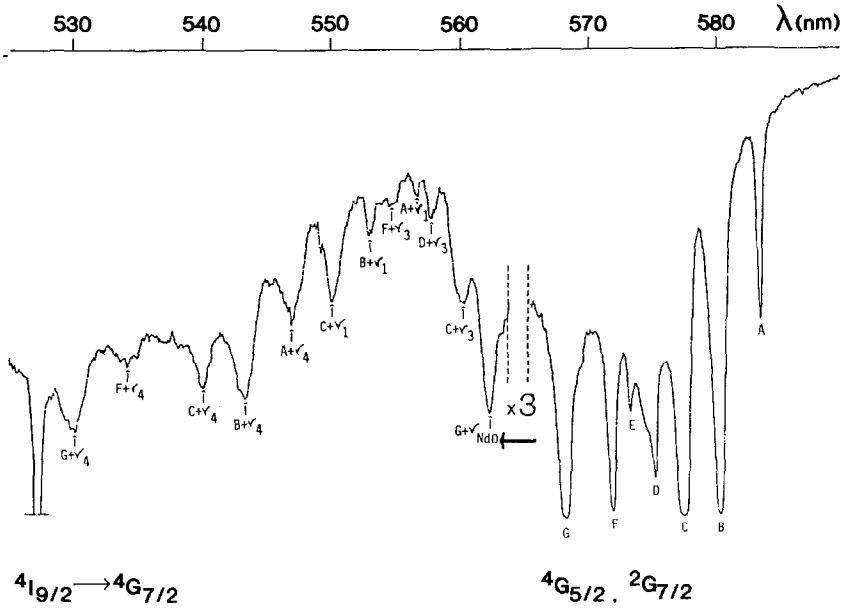

FIG. 3. Part of the absorption spectrum of $NdBO_3$ at 4.2 K in the hypersensitive transition area (arrows indicate the vibronic replica and their assignment).

TABLE I

ENERGY OF ABSORPTION LINES OF $NdBO_3$ IN THE REGION OF HYPERSENSITIVE TRANSITION

Energy	Assignment: Electronic level	Assignment: Vibrational mode
17,027	$^4G_{5/2}$ A	
17,142	$^4G_{5/2}$ B	
17,246	$^4G_{5/2}$ C	
17,329	$^4G_{7/2} + {}^2G_{7/2}$ D	
17,393	$^4G_{7/2} + {}^2G_{7/2}$ E	
17,441	$^4G_{7/2} + {}^2G_{7/2}$ F	
17,583	$^4G_{7/2} + {}^2G_{7/2}$ G	
17,779	$G + 196^a$	ν (Nd–O)
17,856	$C + 610$	ν_3 (B–O)
17,934	$D + 605$	ν_3 (B–O)
17,973	$A + 947$	ν_1 (B–O)
18,032	$F + 591$	ν_3 (B–O)
18,090	$B + 948$	ν_1 (B–O)
18,193	$C + 947$	ν_1 (B–O)
18,296	$A + 1270$	ν_4 (B–O)
18,417	$B + 1275$	ν_4 (B–O)
18,525	$C + 1279$	ν_4 (B–O)
18,711	$F + 1270$	ν_4 (B–O)
18,849	$G + 1266$	ν_4 (B–O)

Note. All values in cm^{-1} units.

[a] Frequency value near that observed for $^2P_{1/2}$ level.

and γ) and the six three-body (Judd's) parameters T^λ (*15*). The other magnetic parameters P^k and M_k are not included. The Hamiltonian is written

$$H_{FI} = H_0 + \sum_{k=0\to4} e_k \cdot E^k + \zeta_{4f} A_{SO} + \alpha L(L+1) + \beta G(G_2) + \gamma G(R_7) + \sum_{\lambda=2\to8\neq5} t_\lambda \cdot T^\lambda.$$

(ii) The crystalline electric field, produced by the surrounding ligands is described by Wybourne's formalism (*16*),

$$H_{CF} = \sum_{k,q} B_q^k (\mathbb{C}_q^k + (-1)^q \mathbb{C}_{-q}^k) + i \cdot S_q^k (\mathbb{C}_q^k - (-1)^q \mathbb{C}_{-q}^k).$$

For the C_s symmetry 15 real (B_q^k) and imaginary (S_q^k) crystal field parameters are involved, but the set can be reduced to 14 by a proper choice of the reference axis system. However, for the successive calculations carried out here, this requires the same choice for the paramagnetic susceptibility calculation.

A simulation involving a relatively low point symmetry is hazardous to carry out, since various sets of crystal field parameters can simulate more or less correctly the data. An calculation of cfps by the "three parameters model" (*17*) does not give trustworthy results as a consequence of the very covalent bonding character. Finally, the simulation was conducted as previously (*18*):

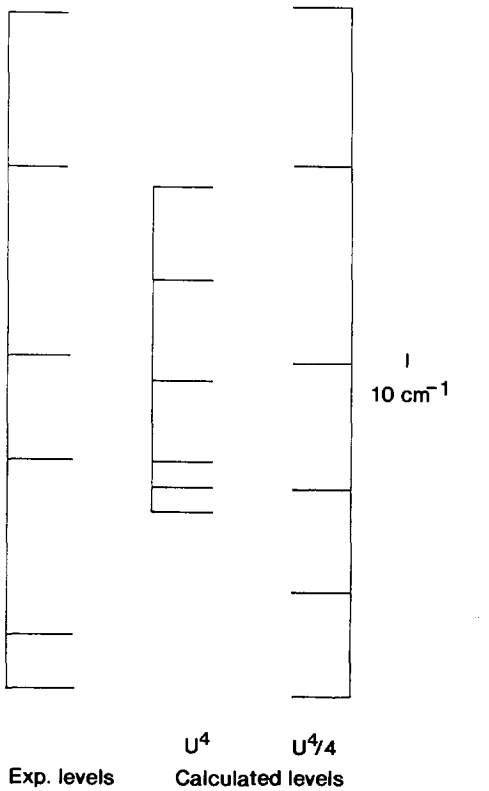

FIG. 4. Comparison of the splitting of the $^2H_{11/2}$ level using different $\langle|U^4|\rangle$ matrix elements with the experimental.

(i) The derived wavefunctions have to reproduce approximately the average paramagnetic susceptibility and its temperature dependency.

(ii) The same cfp set has to simulate another $4f^N$ configuration embedded in an isostructural matrix; in this case $LaBO_3$: Eu^{3+} (*19*).

(iii) The starting values of the free ion parameters are those of $NdAlO_3$, which situates in the same area of the nephelauxetic energy scale (*20*).

The simulation was performed by the program "IMAGE," created for configurations involving complex cfps (*21*). The final rms deviation is 15 cm^{-1}, which is very good for a low symmetry involving 28 phenomenological parameters. Moreover, there is not significant individual mismatch between simulated and observed levels (Table II).

The $^2H_{11/2}$ splitting is not well fitted. This problem has been largely discussed elsewhere by Faucher *et al.* (*22–24*). They remark that compounds where the 4th order crystal field parameter strength is high have the worst simulation of the $^2H_{11/2}$ splitting. They verified phenomenologically that the reduced matrix element $\langle {}^2H2|U^4|{}^2H2\rangle$ divided by a factor 4 improves significantly the simulation. Figure 4 shows the comparison of the $^2H_{11/2}$ splitting by using corrected and original U^4 reduced matrix elements. Another possible reason of the mismatch is the neglect of the $4f^N - 4f^{N-1}5d$ configuration mixing through the odd part of the crystal field potential (*25*).

IV. Paramagnetic Susceptibility

The paramagnetic susceptibility can be calculated by the van Vleck formula, deduced from the perturbation theory,

$$\chi = N\beta^2 \sum_i \left[[E_i^{(1)}]^2/kT - 2E_i^{(2)} \right] B_i,$$

where

$$E_i^{(1)} = \langle \phi_i | L + g_e S | \phi_i \rangle$$

and

$$E_i^{(2)} = \sum_{i \neq j} \frac{\langle \phi_i | L + g_e S | \phi_j \rangle \langle \phi_j | L + g_e S | \phi_i \rangle}{E_i - E_j},$$

where $E_i^{(1)}$ and $E_i^{(2)}$ are the first and second terms of $L + g_e S$, the tensorial operator representing the perturbation of the external magnetic field. N is the Avogadro number, β the Bohr magneton, and B_i the thermal partition. ϕ_i are the unperturbed wavefunctions as obtained from the simulation.

The first term in the expression for χ is temperature dependent, but the second is independent. The latter has the most important contribution to the $4f^6$ configuration (Eu^{3+}), which has a nonmagnetic ground level $^7F_0$, but less important for the other $4f^N$ configurations. Figure 5 shows the comparison between the experimental and calculated values for the average paramagnetic susceptibility (calculations were conducted in the $|{}^4I_J\rangle$ basis, i.e., $E_i < 5000$ cm^{-1}). At low temperatures the agreement is very good, but at higher temperatures a small discrepancy is due to the variation of the crystal field effect with temperature. Free-ion and crystal field parameters for $NdBO_3$ are given in Table III.

V. Conclusion

The absorption spectrum of the neodymium orthoborate $NdBO_3$ was recorded and analyzed at different temperatures. The 119 energy levels could be derived from the electronic transitions within the $4f^3$ configuration. The assignment of the B–O and (Nd–O) vibrational modes accompanying the hypersensitive transition was done, too. The energy level simulation including free ion and crystal field effects (a total of 28 parameters) gave good results (rms deviation equal to 15 cm^{-1}). The B_q^k parameter set is very similar to that derived for the Eu^{3+} ion in the isostructural $LaBO_3$ com-

TABLE II

EXPERIMENTAL AND CALCULATED ENERGY LEVELS OF $NdBO_3$

$^{2S+1}L_J$ level	Exp.	Calc.	ΔE
	0	2	−2
$^4I_{9/2}$	99	108	−9
	145	159	−14
	288	309	−21
	588	594	−6
		2003	
$^4I_{11/2}$		2027	
		2070	
		2096	
		2237	
		2318	
	3957	3952	+5
	3981	3970	+11
$^4I_{13/2}$	4009	4006	+3
	4050	4032	+18
	4184	4187	−3
	4296	4285	+11
	4350	4339	+11
	5845	5849	−4
	5897	5899	−2
	5923	5926	−3
$^4I_{15/2}$	6020	6033	−13
	6265	6260	+5
	6427	6419	+8
	6524	6526	−2
	6621	6612	+9
$^4F_{3/2}$	11,516	11,486	+30
	11,554	11,523	+31
	12,485	12,469	+16
$^4F_{5/2}$, $^2H_{9/2}$	12,523	12,514	+9
	12,601	12,599	+2
	12,630	12,619	+11
	12,665	12,662	+3
	12,728	12,723	+5
	12,804	12,844	−40
	12,872	12,902	−30
	13,424	13,431	−7
$^4F_{7/2}$, $^4S_{3/2}$	13,512	13,530	−18
	13,553	13,588	−35
	13,620	13,615	+5
	13,620	13,623	−3
	13,676	13,674	+2
	14,709	14,710	−1
	14,762	14,751	+11

TABLE II—*Continued*

$^{2S+1}L_J$ level	Exp.	Calc.	ΔE
$^4F_{9/2}$	14,832	14,836	−4
	14,874	14,881	−7
	14,912	14,940	−28
	15,899	15,887	+12
	15,918	15,923	−5
$^2H_{11/2}$	15,978	15,958	+20
	16,014	16,002	+12
	16,080	16,071	+9
	16,134	16,126	+8
	17,027	17,031	−4
	17,142	17,139	+3
$^4G_{5/2}$, $^2G_{7/2}$	17,246	17,224	+22
	17,329	17,352	−23
	17,393	17,406	−13
	17,441	17,426	+15
	17,583	17,567	+16
	18,934	18,915	+19
$^4G_{7/2}$	19,027	19,018	+9
	19,075	19,070	+5
	19,143	19,132	+11
	19,343	19,346	−3
	19,467	19,475	−8
$^4G_{9/2}$, $^2K_{13/2}$	19,504	19,513	−9
	19,533	19,538	−5
	19,589	19,576	+13
	—	19,599	—
	19,621	19,634	−13
	—	19,709	—
	19,734	19,745	−11
	19,796	19,793	+3
	19,864	19,843	+21
	19,964	19,948	+16
	20,972	20,959	+13
	20,982	20,993	−11
	21,008	21,027	−19
	21,039	21,043	−4
	21,112	21,105	+7
	21,158	21,141	+17
	21,230	21,238	−8
	21,337	21,349	−12
$^2G_{9/2}$, $^4G_{11/2}$,	21,420	21,443	−23
$^2D_{3/2}$, $^2K_{15/2}$	21,468	21,471	−3
	—	21,576	—
	21,614	21,610	+4
	21,646	21,668	−22
	21,700	21,717	−17
	21,750	21,743	+7
	21,773	21,795	−22

TABLE II—*Continued*

$^{2S+1}L_J$ level	Exp.	Calc.	ΔE
	21,806	21,811	−5
	—	21,836	—
	21,878	21,864	+14
	21,906	21,892	+14
	21,953	21,953	0
$^2P_{1/2}$	23,310	23,314	−4
	23,830	23,834	−4
$^2D_{5/2}$	23,883	23,883	0
	23,933	23,933	0
$^2P_{3/2}$	26,173	26,176	−3
	26,248	26,243	+5
$^4D_{3/2}$	27,965	27,953	+12
	28,052	28,038	+14
	28,182	28,178	+4
$^4D_{5/2}$	28,317	28,328	−11
	28,458	28,449	+8
$^4D_{1/2}$	28,630	28,643	−13
	29,063	29,052	+11
	29,171	29,189	−18
$^2I_{11/2}$	29,248	29,257	−9
	29,406	29,405	+1
	29,522	29,509	+13
	29,543	29,548	−5
	30,008	30,007	+1
	30,108	30,092	+8
	30,126	30,135	−9
$^4D_{7/2}$, $^2L_{15/2}$, $^2I_{13/2}$	30,168	30,167	+1
	—	30,189	—
	30,259	30,274	−15
	30,301	30,316	−15
	—	30,327	—
	—	30,348	—
	30,393	30,389	+4
	—	30,453	—
	—	30,508	—
	30,521	30,523	−2
	—	30,631	—
	30,670	30,677	−7
	30,784	30,784	0
	30,847	30,824	+23
	30,881	30,881	0
	—	30,902	—
	—	31,565	—
	—	31,625	—
$^2L_{17/2}$	31,667	31,663	+4
	31,690	31,689	+1

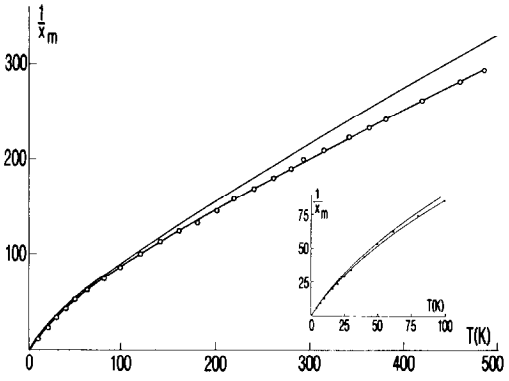

FIG. 5. Experimental and calculated paramagnetic susceptibility of $NdBO_3$ between 4.2 and 500 K.

TABLE III

FREE-ION AND CRYSTAL FIELD PARAMETERS FOR $NdBO_3$ (AND FOR $LaBO_3:Eu^{3+}$ (*19*))

Parameter	$NdBO_3$		$LaBO_3:Eu^{3+}$
E^0	13,076	±1	
E^1	4959	±0.5	
E^2	23.4	±0.01	
E^3	486	±1	
α	21.1	±0.5	
β	−619	±1	
γ	[747]		
T^2	234	±2	
T^3	41	±2	
T^4	79	±2	
T^6	−270	±5	
T^7	283	±5	
T^8	337	±9	
ζ	875	±1	
B_0^2	11	±14	−28
B_2^2	−228	±8	−231
S_2^2	0		0
B_0^4	−781	±33	−501
B_2^4	187	±34	172
S_2^4	−218	±34	−164
B_4^4	−338	±39	−318
S_4^4	1247	±14	935
B_0^6	879	±42	975
B_2^6	−279	±36	−292
S_2^6	−747	±24	−677
B_4^6	−689	±27	−717
S_4^6	707	±25	337
B_6^6	−84	±29	−14
S_6^6	−51	±33	−179

Note. Number of Stark levels: 119; root mean square deviation (cm^{-1}): 15.0.

pound. The paramagnetic susceptibility calculated on the $|^4I_J\rangle$ basis using the wavefunctions derived from the optical data is in good agreement with the experimental one.

References

1. J. P. Laperches and P. Tarte, *Spectrochim. Acta* **22,** 1201 (1966).
2. J. H. Dennig and S. D. Rosa, *Spectrochim. Acta* **28,** 1775 (1972).
3. J. Hölsä, *Inorg. Chim. Acta* **139,** 257 (1987).
4. A. Wolfert, E. W. J. L. Oomen, and G. Blasse, *J. Solid State Chem.* **59,** 280 (1985).
5. E. M. Levin, R. S. Roth, and J. B. Martin, *Am. Mineral.* **46,** 1030 (1961).
6. R. E. Newham, M. J. Redman, and R. P. Santoro, *J. Am. Ceram. Soc.* **46,** 253 (1987).
7. C. K. Abdullaev, G. G. Dzafarov, and H. S. Mamedov, *Azerb. Khim. Zh. 2.* **3,** 117 (1976).
8. P. E. Caro, *C.R. Acad. Sci. (Paris)* **262,** 992 (1966).
9. P. Porcher and P. Caro, *J. Less-Common Met.* **93,** 151 (1983).
10. E. Antic-Fidancev, M. Lemaitre-Blaise, and P. Caro, *New J. Chem.* **11,** 467 (1987).
11. E. Antic-Fidancev, J. Hölsä, M. Lemaitre-Blaise, and P. Porcher, *J. Phys. Condens. Mater.* **3** (1991), in press.
12. C. K. Jørgensen and B. R. Judd, *Mol. Phys.* **8,** 281 (1964).
13. E. Antic-Fidancev, M. Lemaitre-Blaise, and P. Caro, *C.R. Acad. Sci. (Paris) Ser. II* **298,** 575 (1984).
14. P. Caro, O. K. Moune, E. Antic-Fidancev, and M. Lemaitre-Blaise, *J. Less-Common Met.* **112,** 153 (1985).
15. B. R. Judd and H. Crosswhite, *J. Opt. Soc. Am.* **1,** 255 (1984).
16. B. G. Wybourne, "Spectroscopic Properties of Rare Earths," Wiley, New York (1965).
17. N. Karayanis and C. A. Morrison, Harry Diamond Laboratory Report HDL-TR-1648 (1973).
18. E. Antic-Fidancev, M. Lemaitre-Blaise, P. Porcher, I. Bueno, C. Parada, and R. Saez-Puche, *Inorg. Chim. Acta* **182,** 5 (1991).
19. E. Antic-Fidancev, J. P. Chaminade, M. Lemaitre-Blaise, and P. Porcher, *J. Less-Common Met.*, in press.
20. E. Antic-Fidancev, M. Lemaitre-Blaise, L. Beaury, G. Teste De Sagey, and P. Caro, *J. Chem. Phys.* **73,** 4613 (1980).
21. P. Porcher, Routines REEL and IMAGE for simulating the d^N and f^N configuration involving real (or complex) crystal field parameters, unpublished.
22. M. Faucher, D. Garcia, and P. Porcher, *C.R. Acad. Sci. (Paris) Ser. II* **308,** 603 (1989).
23. M. Faucher, D. Garcia, P. Caro, J. Derouet, and P. Porcher, *J. Phys.* **50,** 219 (1989).
24. M. Faucher, D. Garcia, E. Antic-Fidancev, and M. Lemaitre-Blaise, *J. Phys. Chem. Solids* **50,** 1227 (1989).
25. M. Faucher and D. Garcia, *J. Lumin* **46,** 375 (1990).